Liquid-Liquid Interfacial Areas Formed by Turbine Impellers in Baffled, Cylindrical Mixing Tanks

R. E. ECKERT,
C. M. McLAUGHLIN,
and J. H. RUSHTON

School of Chemical Engineering
Purdue University
West Lafayette, IN 47907

An extensive experimental study on the formation of liquid-liquid interfacial areas was conducted using flat-blade turbine impellers in standard mixing tank geometry. The interfacial areas were measured with a light probe for different combinations of volume fraction, continuous and dispersed phase physical properties, and mechanical mixing conditions.

SCOPE

When two immiscible liquids are combined in a mixing tank, the interfacial area, or drop size, is usually of primary concern. In the operations of extraction, emulsion polymerization, and direct-contact heat transfer, the interfacial area directly affects the rates of interphase mass and heat transfer.

Previous work in liquid-liquid mixing has shown that system variables such as volume fraction of dispersed phase, fluid properties, and the mechanical mixing conditions all have an effect on the interfacial area obtained, but the quantitative relationships have not been well established. Knowledge of these quantitative relationships is extremely important for: (1) the prediction of two-phase interfacial areas in new systems; (2) the optimization of existing operations; and (3) the scale-up of experimental or pilot plant units. Thus, there is a definite need for a better understanding of the liquid-liquid mixing process.

In this study, the principle variables involved in the mixing process were varied systematically in order to identify those factors that have a significant influence on the interfacial area formed. The parameters varied include the volume fraction of dispersed phase, tank size, impeller size, impeller speed, and fluid properties of both the continuous and dispersed phases. Standard mixing tank geometry, baffles, and six-blade, flat-blade turbine impellers were used throughout (Rushton et al., 1950). A light probe described previously (McLaughlin and Rushton, 1973) was used to measure the interfacial areas of the dispersions. A total of 122 different combinations of volume fraction, tank size, impeller size, impeller speed, continuous phase properties, and dispersed phase properties were studied experimentally in a design that enabled interactions as well as functional dependence of the above factors to be determined. In addition, 42 replicated runs of these conditions were used to strengthen the determined functional dependence of interfacial area on the above factors and establish the statistical validity of this model.

CONCLUSIONS AND SIGNIFICANCE

Our detailed experimental study of liquid-liquid mixing with flat-blade turbine impellers in standard mixing tank geometry has shown that the interfacial area per unit volume of dispersion is primarily a function of seven variables: Φ, σ, μ_d, ρ_d, ρ_c, P/V and U. Furthermore, statistical regressions on the experimental data identified those variables that significantly affect the area of the dispersions in a mixing tank. The results are presented as regression equations that represent the effects of the mixing parameters far more accurately than previously reported studies, wherein dimensionless groups, such as the Weber number, were relied upon. Furthermore, it was found that the interactions between some of these parameters are highly significant, which explains in part why previous works in this field have often been contradictory.

For purposes of comparison with previous work, some of the significant interactions can be neglected. The resulting equation is not as good a prediction of interfacial area but does enable a direct comparison with previous work in which there were insufficient data to evaluate interactions. Our simplified model for interfacial area has an exponent of 0.66 on volume fraction, while the average of six previous studies reporting such a value

Correspondence concerning this paper should be addressed to Roger E. Eckert.
Craig M. McLaughlin is with Texaco, Inc., Houston, Texas 77052.

is 0.78. Our exponents on the impeller diameter and impeller speed are 1.23 and 1.11, respectively, for geometrically similar systems; the values compare extremely well with previous works.

INTRODUCTION

In a recent book, Oldshue (1983) reviews liquid-liquid mass transfer and presents some of the models used to express Sauter-mean diameter of the dispersed drops as functions of the agitation factors. Studies of liquid-liquid interfacial areas in mixing tanks have also been summarized in tables by both Fernandes and Sharma (1967) and Coulaloglou and Tavlarides (1976). These extensive tables include the range of experimental conditions studied, the type of impeller, and the method used for measuring interfacial area. Paddle agitators were used by Vermeulan et al. (1955) and Kagan and Kovalev (1966), while the propeller-type was used by Pavlushenko and Yanishevskii (1958, 1959). Turbines were employed in the work of Rodger, et al. (1956) and by Yamaguchi et al. (1963). Investigators who compared these types of agitators are Kafarov and Babanov (1959), Rodriguez et al. (1961), and Fernandes and Sharma (1967).

The most common experimental methods of measuring interfacial area are light transmission and photography. Sprow (1967a,b) used a Coulter counter for strongly coalescing systems. In general these studies were conducted in batch-type mixing tanks, but continuous systems were used by Thornton and Bouyatiotis (1963), Bouyatiotis and Thornton (1967), Keey and Glen (1969), Schindler and Treybal (1968), Weinstein and Treybal (1973), and Coulaloglou and Tavlarides (1976).

Most works correlated experimental data by expressing interfacial area as a product of agitator speed, tank diameter, fraction of dispersed phase, and Weber number, each to a power determined empirically. However, there has been little agreement on the quantitative values of the exponents in these relationships. For example, the exponent of Φ varies from -0.53 to 1.0, and the exponent of D varies from 0.7 and 2.0. Such lack of ageement is likely because of the complexity of the break-up and coalescence process in the mixing tank, and the necessity of expressing this complex process in terms of a simplified mathematical model. Shinnar and Church (1960) and Shinnar (1961) present a theory that dispersions are stabilized by the mixing turbulence; the exponents on various factors have been discussed in light of theory (Coulaloglou and Tavlarides, 1976).

A model for the Sauter mean diameter used frequently is of the form

$$\frac{d_{32}}{D} = b(1 + c\Phi)N_{we}^{-0.6} \tag{1}$$

Equation 1 is used by Calderbank (1958), Chen and Middleman (1967), Brown and Pitt (1970), Mlynek and Resnick (1972), and Coulaloglou and Tavlarides (1976) with values of b ranging from 0.058 to 0.081, and values of c from 3.14 to 9. In a following study Brown and Pitt (1974) chose a different form of model for the Sauter mean diameter. Skelland and Lee (1978, 1981) developed a correlation that has the 1.4 power on Reynolds number, 0.7 on D/T, -0.53 on Φ, and does not depend upon the Weber number.

"There are large differences in the interfacial area data by different investigators," notes Oldshue (1983), and he concludes, "they are probably not adequate for use as absolute data." Most of the previous studies have not varied all the important parameters in a comprehensive plan. Such approaches can be misleading because the volume fraction, fluid properties, and mixing conditions surely interact with one another in affecting the drop size or interfacial area.

The purpose of this work was a detailed study of the most efficient system geometry for obtaining high interfacial areas. Previous work by Rushton et al. (1950) and Rushton and Oldshue (1959) showed that a cylindrical tank with four equally-spaced wall baffles, each one-tenth of the tank diameter in width, is desirable for this type of operation. This standard configuration was used, with the liquid depth equal to the tank diameter, and the impeller placed at one-third off-bottom. For liquid-liquid mixing, this impeller location seems to be better than the more commonly reported one-half off-bottom position because no sacrifice is made in interfacial area (Fernandes and Sharma, 1967) and more power can be exerted on the two liquids before air is entrained into the system. Geometrical similarity was maintained in all dimensions except for impeller size to lend direct applicability to scale-up procedures (Rushton, 1951).

The impeller type used was a six-flat-blade turbine because this impeller has given the best results when dealing with liquid-liquid systems (Fernandes and Sharma, 1967; Pitt, 1966). With a given tank geometry and liquid pair the flat-blade turbine is generally most efficient in creating the maximum interfacial area (minimum drop size) for a given power input and impeller diameter. For this reason the standard six-flat-blade turbine (Rushton et al., 1950) was used in all experiments. Figure 1 illustrates the basic tank geometry used, with the flow lines from the turbine impeller indicated by the arrows.

In a baffled cylindrical tank with a turbine impeller, there are numerous parameters that could significantly affect the interfacial area per unit volume of dispersion, a. Some of the most obvious are the volume fraction Φ, the impeller diameter D, the impeller speed N, the tank diameter T, the interfacial tension between the two fluids σ, the continuous phase viscosity, μ_c, and density ρ_c, and the dispersed phase viscosity μ_d, and density ρ_d. Other possibly variables directly related to the above nine include the ratio of impeller diameter to tank diameter D/T, the power per unit volume exerted on the fluids P/V, the impeller Reynolds' number N_{Re}, the impeller tip speed U, and the Weber number N_{We}.

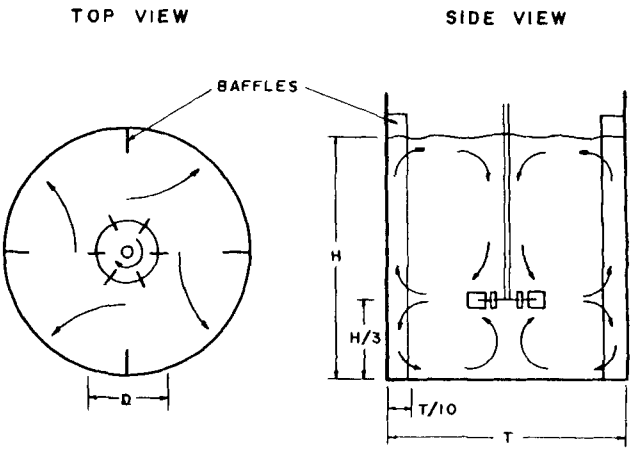

Figure 1. Mixing tank geometry studied.

TABLE 1. EXPERIMENTAL LEVELS, DESIGN I

Variable	Units	Levels						
		Low_4	Low_3	Low_2	Low_1	Middle	$High_1$	$High_2$
Φ	(dimensionless)	—	—	0.005	0.01	0.02	0.04	0.08
σ	dynes/cm (10^{-5} N/cm)	8.6	14.3	24.4	37.4	39.0	41.6	52.5
T	cm	—	—	—	14.2	29.5	43.9	—
D/T	(dimensionless)	—	—	—	1/3	5/12	1/2	—
N	s^{-1}	—	—	—	N_1	N_2	N_3	—

EXPERIMENTAL DESIGN AND METHOD

The purpose of the experimental design was twofold: to identify the significant variables, and to quantify the effects of these variables. To accomplish these purposes the experimental design was divided into two parts. In the first part (design I), the continuous phase was water, and the properties of the dispersed phase were varied by using different organic liquids. In the second part (design II) the properties of the continuous phase were varied by the addition of various amounts of corn syrup to the water phase, while the properties of the dispersed phase were again varied.

For design I the independent variables are Φ, σ, T, D/T, and N; combination variables vary as a result of changing these five factors. For three levels each, five factors require 243 treatment combinations if a full factorial design is used, so a modified central composite design (Davies, 1963) was chosen to substantially reduce the size of the experimental design. In this design, seven levels of σ, five levels of Φ, and three levels each of T, D/T, and N were studied. The levels of each factor in the design are summarized in Table 1. The different levels of σ were obtained by using different organic liquids as the dispersed phase. Where possible, the different levels were equally spaced on a logarithmic scale (Φ, for example), because of the form of the mathematical model (see the Regression Analysis section). In the table, the exact levels of N cannot be specified because they varied with each combination of the previous variables. The impeller speed for each set of conditions must be great enough so that all the organic phase is dispersed, but not so great that air is drawn into the system. The presence of air bubbles in the system is generally undesirable, and interferes with the light transmission technique for measuring the interfacial area. The range of impeller speeds for all runs is 1.33 to 11.67 s^{-1}.

The physical properties of the organic liquids used to obtain the various levels of σ are given in Table 2. The interfacial tension listed is that of the mutally saturated organic-water pair. As shown, the interfacial tension was varied from 8.6 to 52.5 dyne/cm (10^{-5} N/cm), the dispersed phase viscosity from 0.445 to 129.0 mPa·s, and the dispersed phase density from 0.714 to 1.20 g/cm^3. These experimentally determined values were obtained as described in the Experimental Methods section. Literature values were available at 20°C for many of these properties and are given for comparison only.

The modified central composite design resulted in 27 different combinations of Φ, σ, T, and D/T. Three or more impeller speeds for each combination of Φ, σ, T, and D/T led to a study of 85 different combinations of the independent variables. To allow the estimation of the experimental error, 23 of these 85 combinations were replicated at least once for a total of 114 trials.

After completion of this experimental design, it was thought that the impeller Reynolds number, $N_{Re} = D^2N\rho_c/\mu_c$, might have a significant effect on the interfacial area. However, only two of the factors in this dimensionless group had been varied, namely D and N. For this reason, an additional experimental design (design II) was formulated to include variation of the density and viscosity of the continuous phase. This was accomplished through the addition of various amounts of corn syrup to the water phase.

For design II, the primary variables are μ_c, Φ, σ, T, D/T, and N. This choice was based on the results of design I, where it was found that Φ, σ, T, D/T, and N all have a significant effect on the interfacial area. Again, a central composite design was performed; the levels of the factors are summarized in Table 3. In this design, levels of σ were obtained with kerosene, xylene, and n-heptane as the dispersed phase, as shown in Table 4. Fewer treatments were required than in design I even though an additional factor had been added, because the effects of Φ, σ, T, D/T, and N were already well established with water as the continuous phase. Design II required the study of 22 different combinations of μ_c, Φ, σ, T, and D/T. Of these 22 combinations, eight had already been studied, because the lower level of μ_c (0.874) is that of water. Thus, only 14 additional combinations of μ_c, Φ, σ, T, and D/T had to be studied. Multiple impeller speeds for each of these combinations gave a total of 37 additional treatments. Finally, 13 of these 37 were replicated, leading to a total of 50 runs for design II.

Upon completion of the two experimental designs, a wide range of laboratory operating conditions had been studied. The ranges of the most prominent variables are listed in Table 5. The table shows that as a result of the mixing conditions studied, the interfacial area per unit volume of dispersion was varied from 2.17 to 19.4 cm^2/cm^3, roughly a tenfold range. The range of Reynolds numbers covered emphasizes the fact that turbulent mixing conditions were maintained in all experiments.

TABLE 2. ORGANIC LIQUIDS USED, DESIGN I (CONTINUOUS PHASE: WATER)

Liquid	σ dynes/cm (10^{-5} N/cm)		μ_s mPa · s		ρ_d g/cm^3	
	20°C*	25°C**	20°C	25°C	20°C	25°C
n-Octanol	8.5	8.6	8.95	7.13	.827	0.825
Oleic acid	15.6	14.3	—	28.7	.854	0.890
Nitrobenzene	25.66	24.4	1.98	1.86	1.205	1.20
Xylene	37.77	37.4	0.65	0.602	0.861	0.860
Kerosene	—	39.0	—	1.32	—	0.796
n-Heptane	—	41.6	0.416	0.445	0.684	0.714
Paraffin oil	—	52.5	—	129.0	—	0.874

* 20°C values from Lange, *Handbook of Chemistry*.
** 25°C is the approximate temperature at which data were determined and runs conducted.

Measurement of Interfacial Area

The impeller was mounted one-third off-bottom in a baffled glass tank. A light probe (McLaughlin, 1970; McLaughlin and Rushton, 1973) was located in the tank so that the optical gap received the discharge of the impeller; the direction of the light beam was perpendicular to the local direction of flow. The gap was located halfway between the impeller tip and the tank wall, where the local direction of flow is approximately 20° in the direction of rotation from the tank diameter (Sachs and Rushton, 1954). The interfacial area at this point is not necessarily equal to the average interfacial area throughout the entire tank because the drops will coalesce as they leave the highly turbulent conditions of the impeller discharge (Hillestad, 1965; Sprow, 1967). Nevertheless, since the interfacial

TABLE 3. EXPERIMENTAL LEVELS, DESIGN II

Variable	Units	Levels		
		Low	Middle	High
ϕ	(dimensionless)	0.01	0.02	0.04
σ*	dynes/cm (10^{-5} N/cm)	35.1	37.4	45.5
μ_c	mPa·s	0.874	1.87	4.00
T	cm	14.2	29.5	43.9
D/T	(dimensionless)	1/3	5/12	1/2
N	s^{-1}	N_1	N_2	N_3

* Varies slightly with μ_c.

TABLE 4. INTERFACIAL TENSIONS FOR ORGANIC LIQUIDS USED, DESIGN II

Liquid	σ at $\mu_c = 1.87$ dynes/cm*	σ at $\mu_c = 4.0$ dynes/cm
Kerosene	35.1	34.9
Xylene	37.4	36.7
n-Heptane	45.5	44.6

* Dynes/cm = 10^{-5} N/cm.

area is measured at the same relative position in each tank size, the results can be applied to the behavior of the average interfacial area as well.

In these experiments the optical gap of the light probe was adjusted so that the fraction of light transmitted for any experiment was greater than 0.10. This assured maximum accuracy in the light transmission measurement, as shown by McLaughlin and Rushton (1973). Drops of diameter less than 0.1 mm can scatter light and cause inaccuracy in determining interfacial area by this method. However, many two-phase dispersions consist of drops above 0.1 mm diameter. For example, Coulaloglou and Tavlarides (1976) used a flash photomicrographic method and a modified dye-light transmission technique to obtain distributions. A typical graph shows negligible volume density of drops near or below 0.1 mm.

The continuous phase was put into the tank and the appropriate volume of dispersed phase (organic) was then added, giving a total liquid depth equal to the tank diameter. The impeller speed was gradually increased until all of the organic phase was drawn off the surface or bottom. Time was allowed for an equilibrium drop size distribution to develop, usually 20 to 30 min. After reaching equilibrium, the voltage developed by the phototube circuit was recorded. Through previous calibration of the light probe with neutral density filters, the voltage reading was translated into the fraction of light transmitted for those experimental conditions. Finally, the interfacial area was calculated with the following equation (McLaughlin and Rushton, 1973):

$$a = \frac{4\ln(f)}{l} \tag{2}$$

When possible, the equilibrium interfacial area was measured for at least three impeller speeds for any particular combination of volume fraction, tank geometry, and liquid pair. This could not be done when the speed range between incomplete dispersion (a stagnant layer of organic on either the surface or bottom) and air entrainment was small. Replicates were performed by repeating the entire experiment, starting with an empty tank, to insure that the overall experimental error was determined.

Measurement of Physical Properties

The physical properties of all fluids used were measured experimentally. The viscosity of each liquid was measured with a Cannon-Fenske viscometer and the density was measured with a standard hydrometer. The interfacial tensions of all the liquid pairs were measured with a DuNouy ring interfacial tensiometer after mutual saturation was achieved.

TABLE 5. RANGE OF VARIABLES STUDIED

Variable	Minimum	Maximum	Units
a	2.17	19.40	cm^2/cm^3
ϕ	0.005	0.08	(dimensionless)
T	14.2	43.9	cm
D/T	0.34	0.54	(dimensionless)
N	1.33	11.67	s^{-1}
σ	8.6	52.5	dynes/cm (10^{-5} N/cm)
μ_d	0.445	129.0	mPa·s
ρ_d	0.714	1.20	g/cm^3
μ_c	0.874	4.05	mPa·s
ρ_c	0.996	1.140	g/cm^3
P	8,100	428,300	g·cm/s
P/V	1.32	17.42	g/cm^2·s
N_{Re}	7,200	114,700	(dimensionless)
N_{We}	137	1,528	(dimensionless)
U	80	207	cm/s

REGRESSION ANALYSIS

The overall model expresses interfacial area as a product of various functional forms for each factor and interactions of two factors. For example the functional groups used for phase ratio Φ alone included Φ^w, $(1-\Phi)^x$, $y \ln\Phi$, $e^{z\Phi}$ and all possible combinations of these four, where w, x, y, and z are constants. Statistical regression calculations were performed on the logarithm of interfacial area which transforms the terms of the equation from a multiplicative to an additive model.

A total of 64 terms were used as candidates for the equation in a stepwise sequential addition of significant terms or "build-up" regression procedure. For example, the term $\ln\Phi$ was often first placed in the model because it formed the best one-term model. Then the second term, usually $\ln\sigma$, was selected for its greatest further contribution of remaining terms to predicting area, and so on. Terms could also be deleted; after other terms entered the equation a term would be removed if it no longer significantly contributed to prediction.

RESULTS

Over fifty regressions were performed using the experimental data. With an alpha risk of 0.01 (i.e., all terms in the equation are significant at the 99% level) the best model is the following 18-constant equation:

$$a = 0.186\Phi^{\alpha}\sigma^{\beta}\mu_d^{\gamma}\rho_c^{\delta}\rho_d^{-0.71}\left(\frac{P}{V}\right)^{\epsilon}u^{\eta} \tag{3}$$

where

$$\alpha = 1.54 + 0.12\ln(\Phi) + 0.15\ln(\mu_d)$$

$$\beta = 5.77 - 1.04\ln(\sigma)$$

$$\gamma = 0.74 - 0.03\ln(\mu_d)$$

$$\delta = 78.6 - 22.5\ln(\sigma) - 6.93\ln(\mu_d)$$

$$\epsilon = 0.68 + 0.08\ln(\Phi) - 0.10\ln(P/V)$$

$$\eta = 1.35 + 0.12\ln(\mu_d) - 0.73\ln(u)$$

In this equation, the tip speed divided by 100, u, is used rather than the actual tip speed U, for scaling convenience. The equation accounts for 92.3% of the sum of squares of $\ln a$ around its average; this is an overall measure of the fraction of the variation in the response that is accounted for by the model. Equation 3 does have significant lack of fit, but this is attributed to the restrictions of the basic multiplicative model, and not to any theoretical oversights in the terms considered. Since the form of the model is empirical instead of theoretical, the lack of fit is not surprising. Actually, some equations were found that did not have significant lack of fit, but the number of terms needed for these (above 30) was excessive for convenient use.

Candidate factors and higher terms considered but not selected by using this stepwise regression procedure included impeller speed N, impeller diameter D, tank diameter T, the squares of each of these three, and interactions of among these factors and also with Φ and σ. Furthermore, the Reynolds and Weber numbers based on both pure phase properties and averaged properties, ND^3 (bulk

flow), P, and D/T were likewise rejected. Many of the factors where also tried in nonlogarithmic form, which would lead to exponential terms in the direct interfacial area prediction equation, but none of these appear in the equation. Note that when a square or interaction term was added to the equation the corresponding linear term was included to avoid unwarranted restrictions on the empirical model.

The most noticeable aspect of this form of the equation is the large amount of interaction between the fluid properties, volume fraction, and mixing conditions. For example, the effect of volume fraction on the interfacial area depends in part on the dispersed phase viscosity. Likewise, the effect of the power per unit volume depends on the volume fraction. From these results it is not surprising that previous works have been contradictory, because all seven of the parameters in the equation have not been varied in a single study to determine interactions. It is interesting that only these seven parameters enter the equation, considering that over 20 theoretical parameters, including dimensionless groups, were tested. Apparently the influence of those factors not in the equation, such as N_{Re} and N_{We}, is accounted for in other ways.

Unexpectedly, the influence of the mechanical mixing conditions is described fully by only two parameters, the tip speed U and the power per unit volume exerted on the fluids, P/V. This implies that the effects of the impeller speed, impeller size, and tank size are due solely to their contributions to the tip speed and power per unit volume in liquid-liquid mixing. The parameters N, D, and T, are the parameters most commonly used to describe the mechanical mixing conditions, and are related to the tip speed and power per unit volume by

$$U = \pi ND \tag{4}$$

and

$$P/V = \frac{4K_1\rho_c N^3 D^5}{g_c \pi T^3} \tag{5}$$

where $K_1 = 6.3$ for a six-flat-blade turbine under turbulent mixing conditions (Rushton et al., 1950).

As can be seen in Eq. 3, no dimensionless groups have been included except for the volume fraction, which is dimensionless by definition. This is contrary to most previous works, but the correlations in these works were invariably forced into a dimensionless form. Previous works have usually relied on the dimensionless Weber number to account for the effect of the fluid properties. Dimensionless correlations of the experimental data were attempted in this work, but never was the fit as good as that of a similar number of dimensional terms. Thus, it does not appear that a description of this system can be simplified to an equation that involves only dimensionless numbers.

The purpose of this study includes prediction of interfacial surface area per unit volume as a function of the seven factors of Eq. 3. The graphs presented are two-dimensional "cuts" through the eight-dimensional space showing the dependence of this response on one or two of the factors. The 164 data points are spread systematically in the seven factor dimensions according to the previously described experimental designs. Specific data points are not generally located on these "cuts" through the high-dimensional space. For example, impeller speeds could not be fixed at predetermined levels as they were governed by the limits between entrainment and dispersion of all the organic, as previously described. Power per volume is a factor, but measured values that were not initially designed had to be used. In graphs it is necessary to fix most of the seven factors at specific values to show the effects of one or two. Those data points located on or near the graphs are insufficient to display the multidimensional relationship of the equation. Therefore data points are not shown on the graphs. Deviations of the data from the predicted response are taken into account by the statistically calculated confidence interval, which can be visualized as the region between hyperplanes that we are quite certain contains the true interfacial area per unit volume. The locations of these planes are indicated by tick-marks below and above some predicted response lines; these are the 90% confidence limits on a. Only typical values are given to avoid confusion with the other lines on the graphs.

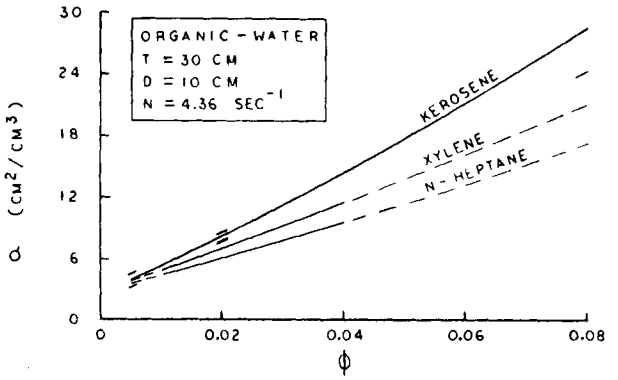

Figure 2. Effect of volume fraction on interfacial area at typical mixing conditions. Tick-marks below and above predicted response lines are 90% confidence intervals on *a*.

To discuss the effects of the most important variables, the interfacial area can be thought of as a function of three collections of effects: the volume fraction, the fluid properties, and the mechanical mixing conditions.

Effect of Volume Fraction

As was previously mentioned, the effect of the volume fraction on the interfacial area depends on the viscosity of the dispersed phase as well as its volume fraction. Figure 2 shows interfacial area for varying volume fractions of three fluids, xylene, n-heptane, and kerosene, under typical mixing conditions. The solid lines indicate where experimental data were obtained, and the dashed line-sections are extrapolations based on the regression equation. Since the lines are not parallel, the effect of volume fraction interacts with the physical properties, as all other conditions are constant in this plot. The 90% confidence limits for the kerosene curve are shown

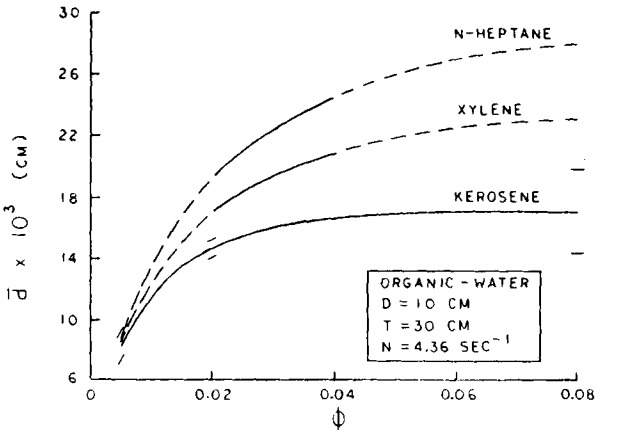

Figure 3. Effect of volume on Sauter mean diameter at typical mixing conditions. Tick-marks below and above predicted response lines are 90% confidence intervals on *a*.

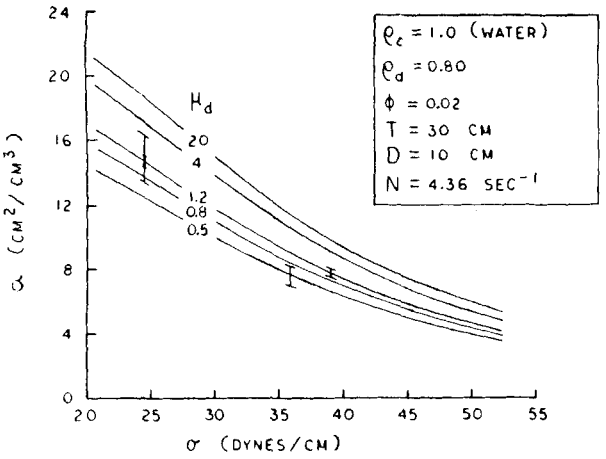

Figure 4. Effect of σ and μ_d on interfacial area at typical mixing conditions. Tick-marks below and above predicted response lines are 90% confidence intervals on *a*.

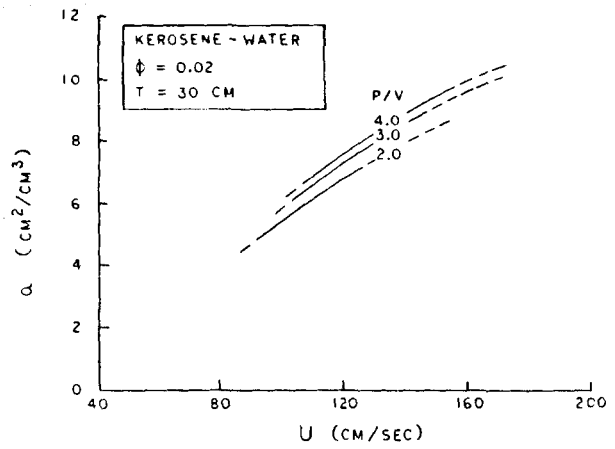

Figure 6. Effect of *U* on interfacial area at different levels of *P/V*.

by the tick marks at volume fractions of 0.005, 0.02, and 0.08. (These marks indicate the 90% confidence limits in all figures.) The confidence limits show that the precision of the regression equation is best at the intermediate values of Φ, and decreases as the extremes are approached.

The effect of the volume fraction can also be illustrated by Figure 3, where the Sauter mean diameter is plotted against the volume fraction for the same fluids and same mixing conditions as those of Figure 2. The Sauter mean diameter is an area-average diameter for the dispersion, and is directly related to the interfacial area by

$$d_{32} = \frac{6\Phi}{a} \tag{6}$$

Figure 3 shows that increases in the volume fraction of dispersed phase leads to increases in the Sauter mean diameter at the lower volume fractions. This implies that at the lower volume fractions, an increase in the amount of dispersed phase contributes more to the rate of drop coalescence than it does to the rate of drop break-up. Therefore, the drop size increases as the volume fraction increases in this region. These curves level off at higher volume fraction because the rates of coalescence and break-up both contribute in this region, which agrees with the findings in many previous works. This effect of volume fraction is not to be confused with the fact that, for any fixed volume fraction, an equilibrium drop size distribution will develop because the rates of break-up and coalescence eventually become equal.

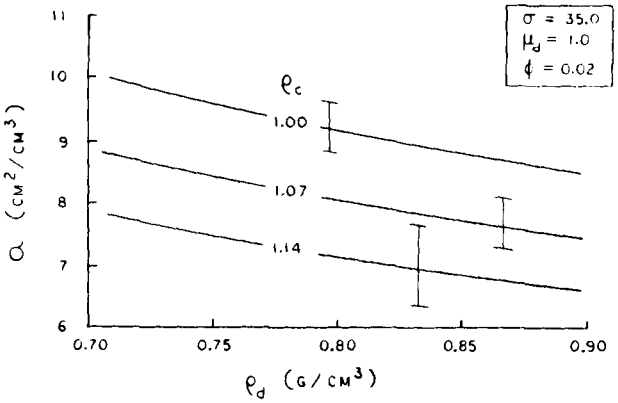

Figure 5. Effect of ρ_c and ρ_d on interfacial area at typical mixing conditions. Tick-marks below and above predicted response lines are 90% confidence intervals on *a*.

Effect of Fluid Properties

The fluid properties are very important in determining the interfacial area of a liquid-liquid system, as exhibited by the inclusion of σ, μ_d, ρ_d, and ρ_c in the regression equation. The most significant of these four are σ and μ_d; Figure 4 shows the effect of these two factors at typical values of the others. Interfacial area is increased by a decrease in the interfacial tension. The interfacial tension is a measure of the resistance to break-up, and a decrease in this resistance will cause the drop size to decrease. The interfacial area increases with increasing viscosity of the dispersed phase. A higher viscosity allows the fluid shear to be transmitted more easily, leading to smaller drops and a higher interfacial area.

The influence of the dispersed and continuous phase densities are illustrated in Figure 5 for typical values of all the other parameters. Interfacial area is increased by a decrease in the dispersed phase density. This trend seems reasonable because a decrease in ρ_d, while holding μ_d constant will cause the kinematic viscosity of the dispersed phase to increase. An increase in the kinematic viscosity allows the shear to be transferred more readily, leading to smaller drops and larger interfacial area. The same analysis holds for the effect of ρ_c, because lower densities lead to higher interfacial areas in this case also. In addition, it can be reasoned that denser fluids require more power for the same fluid motion, making less energy available for drop break-up.

Effect of Mixing Conditions

It has already been stated that the effect of the mixing conditions can be summarized by only two variables, the tip speed U and the power per unit volume exerted on the fluids, P/V. Of these two, the tip speed is far more important, as illustrated in Figure 6, which shows how the interfacial area is affected by U and P/V for a kerosene-water system in a 30 cm tank with $\Phi = 0.02$. If the conditions of $U = 107$ cm/s and $P/V = 2.0$ g/cm^2·s (or 1.0 hp/1,000 gal) are taken as a basis, the interfacial area is 14% higher for either of the following:

1. A 100% increase in the power input with the same tip speed.

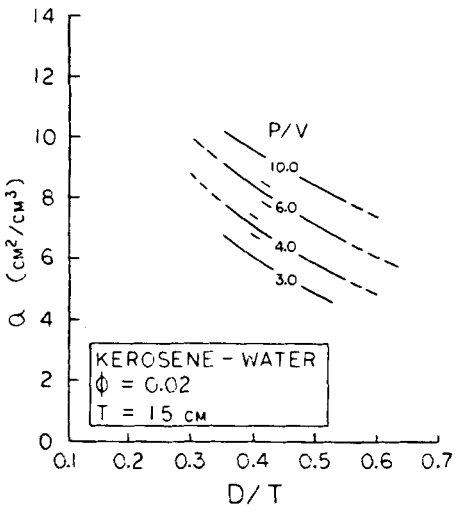

Figure 7. Effect of *D/T* on interfacial area at different levels of *P/V*, kerosene-water, 15 cm tank. Tick-marks below and above predicted response lines are 90% confidence intervals on *a*.

2. A 9% increase in the tip speed at the same power input.

Thus, the tip speed has a much larger effect on the interfacial area than does the specific power input. Although this example is at specific conditions of volume fraction, tank size, and fluid properties, the controlling influence of U (rather than P/V) was found at all other conditions as well. Therefore, the effect of N and D is more closely approximated by the product ND, which is proportional to U, rather than the product N^3D^5, which is proportional to P/V.

The dependence of the interfacial area on the mixing conditions can be summarized by the parameters D/T, P/V, and T. The effects of D/T and P/V are shown in Figure 7 for the kerosene-water system ($\Phi = 0.02$) in the 15 cm tank. Extrapolations to larger D/T ratios beyond the range indicated for each level of P/V are not valid because air is entrained at these conditions. Similarly, the lower limits of D/T on each P/V curve indicate the approximate point at which a stagnant layer of organic develops. The minimum speeds required for complete dispersion have been studied by Pavlushenko and Yanishevskii (1958). The experimental data indicated that levels of P/V far outside the range from 3.0 to 10.0 g/cm²-s (or 1.5 to 5.0 hp/1,000 gal) would not produce acceptable dispersions in this tank size, no matter what the D/T ratio.

The most interesting deduction to be made from Figure 7 is that within the operable range, smaller ratios of impeller diameter to tank diameter always produce higher interfacial areas at a given power input. Since smaller values of D/T give higher ratios of turbulence to bulk flow at the same power input, the formation of interfacial areas must be favored by conditions of high turbulence. Thus, the creation of liquid-liquid interfacial areas is a "turbulence-controlled" process, as proposed by Rushton and Oldshue (1959). It can also be deduced that a decrease in D/T will produce the same interfacial area at a fraction of the original power input. As an example, a 15 cm tank with $D/T = 0.35$ and $P/V = 3.0$ g/cm²-s (1.5 hp/1,000 gal) will produce the same interfacial area as a system with $D/T = 0.55$ at twice the power input.

Figures 8 and 9 show the same general relationship for two other tank sizes: 30 and 45 cm in diameter. Note that lower levels of P/V are adequate to achieve the same interfacial area at the same D/T ratio in larger tanks. At a D/T value of 0.40, a P/V level of 3.0 g/cm²-s (1.5 hp/1,000 gal) is required in the 15 cm tank for an interfacial area of 6.0 cm²/cm³, but the levels of P/V to achieve the same area in the 30 and 45 cm tanks are 1.8 and 1.45 g/cm²-s, respectively.

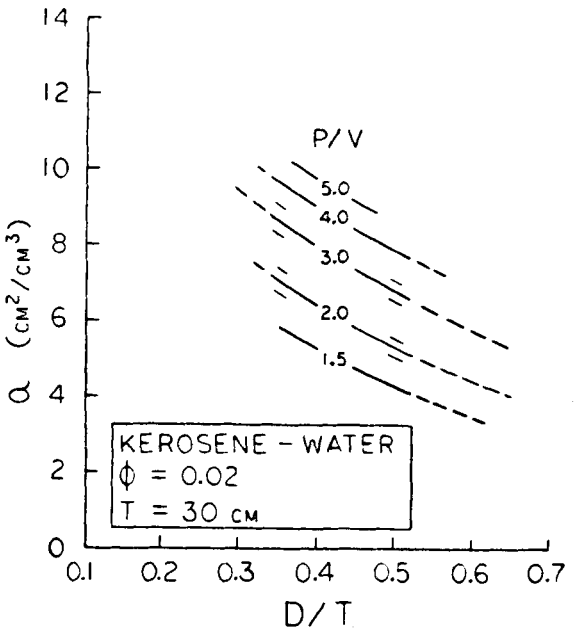

Figure 8. Effect of *D/T* on interfacial area at different levels of *P/V*, kerosene-water, 30 cm tank. Tick-marks below and above predicted response lines are 90% confidence intervals on *a*.

Simplified Regression Equation

While Eq. 3 was found to fit the data quite accurately, it is somewhat complex for many applications. Therefore, a regression was performed in which only eight terms were allowed, seven of which are the first-order terms of Eq. 3. The equation was limited to eight terms because the contributions to better prediction of interfacial area of additional terms dropped markedly. This behavior is basically due to the stepwise regression procedure, where the most significant terms are put into the model first. The result is the following model:

$$a = 0.0364\Phi^{0.66}\sigma^{\alpha}\rho_d^{-0.30}\mu_d^{0.05}\rho_c^{-1.94}(P/V)^{0.06}u^{0.93} \qquad (7)$$

where $\alpha = 5.78 - 1.02\ln(\sigma)$. Eq. 7 accounts for 87.3% of the sum of squares of the response, $\ln a$, about the average, as compared to 92.3% for the 17-term model, Eq. 3. The estimated standard deviation for interfacial area in a single experiment is 8.4% (0.0809 in $\ln a$) for Eq. 7, 27% higher than the value of 6.6% for Eq. 3. Based upon the 42 replicate runs at various conditions the standard deviation is 3.5%.

Presentation of the results in this form allows direct comparison to some previous works which used the model form of exponents on factors and dimensionless groups. The exponent on volume fraction, 0.66, is smaller than the average of the six works reporting such an exponent, 0.78. If Eqs. 4 and 5 are substituted into Eq. 7, the exponents on the impeller diameter and impeller speed are 1.23 and 1.11, respectively, for geometrically similar systems. The first value is the mean of the range (0.5 to 2.0) of literature exponents on D. The exponent on N is essentially identical with the average of reported values for an equation of this form. Finally, when Eq. 1 is expressed for area it always gives powers of 0.8 on D and 1.2 on N, but it is not a direct power function of Φ.

The phenomena studied here are so complex that a rigorous theoretical treatment is impossible. Nevertheless we believe mechanistic modeling can yield insight and is an important direction for future work. In the next section we will describe applications of Eq. 7.

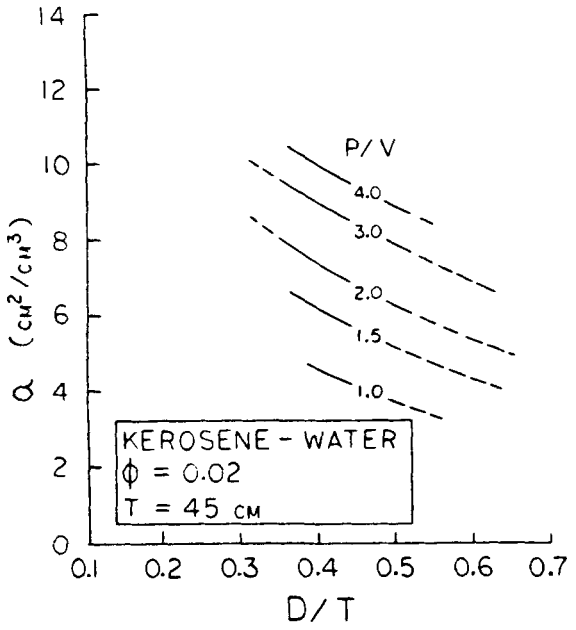

Figure 9. Effect of *D/T* on interfacial area at different levels of *P/V*, kerosene-water, 45 cm tank.

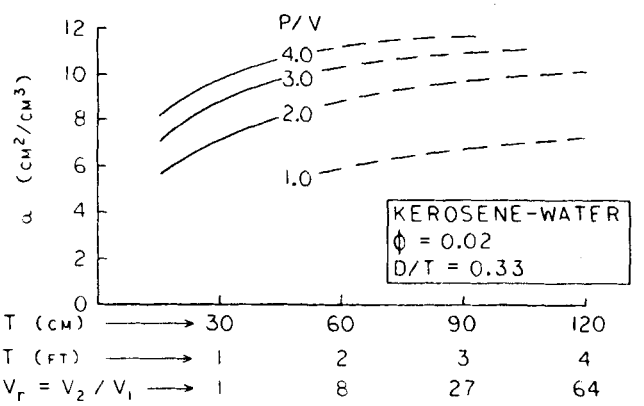

Figure 10. Effect of tank size on interfacial area at constant levels of *P/V*, kerosene-water.

APPLICATION OF THE RESULTS

The results of this work are directly applicable to three engineering problems that can arise when dealing with liquid-liquid interfacial areas in a mixing tank:

1. The prediction of interfacial areas in new systems.
2. The optimization of interfacial areas in existing equipment.
3. The scale-up of interfacial areas when larger systems are desired.

The bearing of this study on each of these is discussed here.

Prediction of Interfacial Areas in New Systems

Equations 3 and 7 are most useful for this purpose; Eq. 3 is more accurate, while Eq. 7 is more easily solved. The required accuracy and the difficulty of the necessary calculations should be the criteria for the choice. In any case, if the conditions to be investigated lie outside of the range of variables studied, both equations should be used with caution. Table 5 lists the range of variables studied in all the experiments, but it must be remembered that these ranges were not explored experimentally in all possible combinations.

Optimization of Interfacial Areas in Existing Equipment

For a specific liquid pair in an existing mixing operation, this work suggests several possible alternatives for maximizing the interfacial area:

1. An increase in the volume fraction of dispersed phase will increase the interfacial area, unless conditions are such that a phase inversion occurs (the dispersed phase suddenly becomes the continuous phase, and vice versa).
2. A decrease in the interfacial tension will increase the interfacial area.
3. For the flat-blade turbine, the smallest diameter for a given power input will produce the maximum interfacial area, if all of the dispersed phase is drawn from the surface or bottom.

Since the volume fraction, fluid properties and mixing conditions interact to such a high degree, it is not possible to associate percentage changes with any of the above except for a particular set of conditions. Nevertheless, application of Eq. 3 will predict the change in area for any given system.

Scale-Up of Interfacial Areas

It is believed that this work will be most useful in the scale-up of mixing systems where the interfacial area is an important consideration. The recommended scale-up procedure is illustrated in Figure 10 where the interfacial area of a kerosene-water mixture is plotted against the tank size for various levels of P/V. For this plot, volume fraction is kept constant at 0.02, and geometric similarity is maintained with $D/T \approx 0.33$ for all tank sizes. The dashed sections of each curve represent extrapolations based on Eq. 3. The plot shows that a constant level of P/V will not give constant interfacial areas as the tank size is increased. If the often-used criterion of constant power per unit volume were applied to this system, large errors could result. For example, experiments in a 30 cm tank with this system at a P/V level of 2.0 g/cm²·s (1.0 hp/1,000 gal) would give an interfacial area of 7.1 cm²/cm³. If constant P/V were used in scaling up to a 120 cm tank, the interfacial area would be 10.1 cm²/cm³, or a 42% increase. Proper scale-up to achieve the same interfacial area would reveal that a P/V level of only 1.0 g/cm²·s is adequate to achieve the same area. Thus, in this case, a linear scale-up of 4.0 (a volumetric scale-up of 64) would require half the specific power input. This type of behavior has been recognized by Fernandes and Sharma (1967), Rushton and Oldshue (1959), and Treybal (1961).

Equation 7 is easily simplified to show the approximate scale-up relationships, so this equation will be discussed here. For a typical scale-up the fluid properties and volume fraction are held constant and Eq. 7 simplifies to

$$a \propto (P/V)^{0.06}(u)^{0.93} \tag{8}$$

or, since $u = U/100$,

$$a \propto (P/V)^{0.06}(U)^{0.93} \tag{9}$$

Equations 4 and 5 for U and P/V can be substituted into this equation to give

$$a \propto N^{1.11}D^{1.23}T^{-0.18} \tag{10}$$

If the subscript 2 refers to the desired conditions in the larger

mixing tank, and the subscript *1* refers to the known conditions in the laboratory or pilot plant, then

$$\frac{a_2}{a_1} = \left(\frac{N_2}{N_1}\right)^{1.11}\left(\frac{D_2}{D_1}\right)^{1.23}\left(\frac{T_2}{T_1}\right)^{-0.18} \tag{11}$$

or

$$a_r = N_r^{1.11} D_r^{1.23} T_r^{-0.18} \tag{12}$$

where $a_r = a_2/a_1$, $N_r = N_2/N_1$, $D_r = D_2/D_1$, and $T_r = T_2/T_1$.

An example of the use of this equation will make its significance more apparent. In a liquid-liquid mass transfer process, the interfacial area is of importance because the rate of transfer is proportional to this area. If it is desired to scale-up such a process to a geometrically similar tank whose diameter is four times that of a smaller unit, then $D_r = 4.0$, $T_r = 4.0$, and

$$a_r = (4.0)^{1.05} N_r^{1.11} = 4.29 N_r^{1.11} \tag{13}$$

This gives the relationship between the speed ratio and interfacial area ratio for the two geometrically similar systems. To achieve the same specific interfacial area in both sizes, $a_r = 1.0$, so $N_r = 0.27$; the impeller speed in the larger unit should be 27% of that in the smaller unit to achieve the same interfacial area per unit volume of dispersion.

Equation 12 can also be applied to systems where geometrical similarity is not maintained. For instance, doubling the tank diameter while keeping the impeller speed and size constant will give

$$a_r = (1)^{1.11}(1)^{1.23}(2)^{-0.18} = 0.882 \tag{14}$$

Likewise, doubling the impeller speed in a given tank would give

$$a_r = (2)^{1.11}(1)^{1.23}(1)^{-0.18} = 2.16 \tag{15}$$

Of course, the basic mixing tank geometry of Figure 1 must be maintained for these results to be valid.

ACKNOWLEDGMENT

Financial support was provided by Purdue University and the American Cyanamid Company. The aid of W. H. Stevenson in the design of the light probe is acknowledged. The authors are indebted to Mixing Equipment Company, Inc. for furnishing equipment used in this study.

NOTATION

a = interfacial area per unit volume dispersion, cm^2/cm^3
b,c = empirically determined constants
d_{32} = Sauter mean diameter of drops, cm
D = diameter of impeller, cm
f = fraction of light transmitted through a dispersion
g_c = gravitational constant
K_1 = proportionality constant for power
l = optical path length, cm
N = impeller speed, rev/s
N_{Re} = impeller Reynolds number, $D^2N\rho_c/\mu_c$
N_{We} = Weber number, $D^3N^2\rho_d/\sigma$
P = power exerted on fluids by impeller, g·cm/s (1.31×10^{-7}hp)
P/V = power per unit volume, $g/cm^2 \cdot s$ (0.499 hp/1000 gal)
T = mixing tank diameter, cm
U = impeller tip speed, cm/s
u = impeller tip speed divided by 100, cm/s
V = volume of the mixing tank, cm^3
w,x,y,z = numerically evaluated constants

Greek Letters

$\alpha,\beta,\gamma,\delta,\epsilon,\eta$ = constants of Eq. 3
μ = viscosity, mPa·s
ρ = density, g/cm^3
σ = interfacial tension, dyne/cm (10^{-5} N/cm)
Φ = volume fraction of dispersed phase

Subscripts

c = continuous phase
d = dispersed phase
e = effective
r = ratio

LITERATURE CITED

Bouyatiotis, B. S., and J. D. Thornton, "Liquid-Liquid Extraction Studies in Stirred Tanks. I: Droplet Size and Holdup," *Inst. Chem. Engrs. (London) Symp. Ser.*, **26**, 43 (1967).

Brown, D. E., and K. Pitt, "Drop Break-Up in a Stirred Liquid-Liquid Contactor," *Proc. Chemeca '70*, Melbourne, Sydney, **83** (1970).

———, "Effect of Impeller Geometry on Drop Break-Up in a Stirred Liquid-Liquid Contactor," *Chem. Eng. Sci.*, **29**, 345 (1974).

Calderbank, P. H., "Physical Rate Processes in Industrial Fermentation. I: The Interfacial Area on Gas-Liquid Contacting with Mechanical Agitation," *Trans. Inst. Chem. Engrs.*, **36**, 443 (1958).

Chen, H. T., and S. Middleman, "Drop Size Distribution in Agitated Liquid-Liquid Systems," *AIChE J.*, **13**, 989 (1967).

Coulaloglou, C. A., and L. L. Tavlarides, "Drop Size Distributions and Coalescence Frequencies of Liquid-Liquid Dispersions in Flow Vessels," *AIChE J.*, **22**, 289 (1976).

Davies, O. L., *The Design and Analysis of Industrial Experiments*, Hafner Pub. Co., New York, 532–537 (1963).

Fernandes, J. B., and M. M. Sharma, "Effective Interfacial Area in Agitated Liquid-Liquid Contactors," *Chem. Eng. Sci.*, **22**, 1267 (1967).

Hillestad, J. G., "A Study of Coalescence Ratio in Mixing Tanks," Ph.D. Thesis, Purdue Univ., Lafayette, IN (1965).

Kafarov, V. V., and B. M. Babanov, "Interfacial Surface of Mutually Insoluble Liquids Produced by Mechanical Mixing with an Impeller," *J. Appl. Chem.* (U.S.S.R.), **32**, 810 (1959).

Kagan, S. Z., and Y. N. Kovalev, "Determination of Interface Area in a Mechanically Mixed, Continuous Liquid-Liquid Flow," *Khim. Prom.*, **42**, 192 (1966).

Keey, R. B. and J. B. Glen, "Area-Free Mass Transfer Coefficients for Liquid Extraction in a Continuously Worked Mixer," *AIChE J.*, **15**, 942 (1969).

McLaughlin, C. M., "Calculation of Interfacial Areas of Dispersions from Simulated Light Transmission Measurements," M.S. Thesis, Chem. Engr., Purdue Univ., Lafayette, IN (1970).

McLaughlin, C. M., and J. H. Rushton, "Interfacial Areas of Liquid-Liquid Dispersions from Light Transmission Measurements," *AIChE J.*, **19**, 817 (1973).

Mlynek, Y., and W. Resnick, "Drop Sizes in Agitated Liquid-Liquid Systems," *AIChE J.*, **18**, 122 (1972).

Oldshue, J. Y., *Fluid Mixing Technology*, McGraw Hill, New York, 243–256 (1983).

Pavlushenko, I. S. and A. V. Yanishevskii, "Effective Number of Revolutions of a Stirrer for the Dispersion of Two Mutually Immiscible Liquids," *Zhur, Priklad, Khim.*, **31**, 1,348 (1958).

———, "Interfacial Surface Area of Mechanically Stirred Mutually Immiscible Liquids," *Zhur, Priklad, Khim.*, **32**, 1,495 (1959).

Pitt, K., "Predicting Interfacial Area in Agitated Liquid-Liquid Systems," *Mutech. Chem. Eng. J.*, **13**, 13 (1966).

Rodger, W. A., V. G. Trice, and J. H. Rushton, "Effect of Fluid Motion on Interfacial Area of Dispersions," *Chem. Eng. Progr.*, **52**, 515 (1956).

Rodriguez, F., L. C. Grotz, and D. L. Engle, "Interfacial Area in Liquid-Liquid Mixing," *AIChE J.*, **7**, 663 (1961).
Rushton, J. H., E. W. Costich, and H. J. Everett, "Power Characteristics of Mixing Impellers," *Chem. Eng. Progr.*, **46**, Pt. I, 395, Pt. II, 467 (1950).
Rushton, J. H., "The Use of Pilot Plant Mixing Data," *Chem. Eng. Progr.*, **47**, 485 (1951).
Rushton, J. H., and J. Y. Oldshue, "Mixing of Liquid," *Chem. Engr. Progr.*, **55**, 181 (1959).
Sachs, J. P., and J. H. Rushton, "Discharge Flow from Turbine-Type Mixing Impellers," *Chem. Eng. Progr.*, **50**, 597 (1954).
Shinnar, R., and J. M. Church, "Predicting Particle Size in Agitated Dispersions," *Ind. Eng. Chem.*, **52**, 253 (1960).
Skelland, A. H. P., and J. M. Lee, "Agitator Speeds in Baffled Vessels for Uniform Liquid-Liquid Dispersions," *Ind. Eng. Chem. Process Des. Dev.*, **17**, 473 (1978).
Skelland, A. H. P., and J. M. Lee, "Drop Size and Continuous-Phase Mass Transfer in Agitated Vessels," *AIChE J.*, **27**, 99 (1981).
Schinder, H. D., and R. E. Treybal, "Continuous-Phase Mass Transfer Coefficients for Liquid Extraction in Agitated Vessels," *AIChE J.*, **14**, 790 (1968).
Sprow, F. B., "Distribution of Drop Sizes Produced in Turbulent Liquid-Liquid Dispersion," *Chem. Eng. Sci.*, **22**, 435 (1967a).
——, "Drop Size Distributions in Strongly Coalescing Agitated Liquid-Liquid Systems," *AIChE J.*, **13**, 995 (1967b).
Thornton, J. D., and B. A. Bouyatiotis, "Liquid Extraction Operations in Stirred Vessels," *Ind. Chem.*, **39**, 298 (1963).
Treybal, R. E., "Stirred Tanks and Mixers for Liquid Extraction," *Ind. Eng. Chem.*, **53**, 597 (1961).
Vermeulen, T., G. M. Williams, and G. E. Langlois, "Interfacial Area in Liquid-Liquid as Gas-Liquid Agitation," *Chem. Eng. Progr.*, **51**, 85-F (1955).
Weinstein, B., and R. E. Treybal, "Liquid-Liquid Contacting in Unbaffled Agitated Vessels," *AIChE J.*, **19**, 304 (1973).
Yagmaguchi, I., S. Yabuta, and S. Nagata, "Interfacial Area in Liquid-Liquid Agitated Systems," *Chem. Eng. (Japan)*, **27**, 576 (1963).

Manuscript received Nov. 28, 1983; revision received Nov. 27 and accepted Dec. 2, 1984.